Nonperturbative dispersive sector in strong (quasi-)Abelian fields

G. Cvetič[a*] and Ji-Young Yu[b†]
[a] *Asia Pacific Center for Theoretical Physics, Seoul 130-012, Korea*
[b] *Department of Physics, Dortmund University, 44221 Dortmund, Germany*

Abstract

In strong (quasi–)Abelian fields, even at the one–loop level of the coupling constant, quantum fluctuations of fermions induce an effective Lagrangian density whose imaginary (absorptive) part is purely nonperturbative and known to be responsible for the fermion–antifermion pair creation. On the other hand, the induced real (dispersive) part has perturbative and nonperturbative contributions. In the one–loop case, we argue how to separate the two contributions from each other for any strength of the field. We show numerically that the nonperturbative contributions are in general comparable with or larger than the induced perturbative ones. We arrive at qualitatively similar conclusions also for the induced energy density. Further, we investigate numerically the quasianalytic continuation of the perturbative results into the nonperturbative sector, by employing (modified) Borel–Padé. It turns out that in the case at hand, we have to integrate over renormalon singularities, but there is no renormalon ambiguity involved.
PACS number(s): 11.15.Bt, 10.10.Jj, 11.15.Tk, 11.80.Fv, 12.20.-m

I. INTRODUCTION

It has been well known for some time that the effects of the fermionic quantum fluctuations in space–time uniform Abelian gauge fields can be effectively integrated out, resulting in a one–loop effective action [1]– [7]. The results have been formulated also for the covariantly homogeneous, thus quasi–Abelian, fields of the $SU(2)$ gauge group [8], and for specific nonhomogeneous magnetic field configurations [9]. All the results can be extended to the case of the quantum fluctuations of scalar particles. The problems arising when genuinely non–Abelian fields with translationally invariant gauge–invariants are present [e.g., in $SU(3)_c$] were discussed, e.g., in Refs. [10,11].

*e-mail: cvetic@apctp.org; address after Sept. 15, 2000: Dept. of Physics, UTFSM, Valparaíso, Chile

†e-mail: yu@dilbert.physik.uni-dortmund.de

The quantum fluctuations of the strong gauge field itself (photons, or gluons) modify additionally those Lagrangian densities induced by the fermionic quantum fluctuations. Such two-loop effects have been successfully derived by Ritus [12] for homogeneous Abelian fields, and further discussed by others [13,14]. In QED, such two–loop effects in the coupling constant change the one–loop result by at most a few per cent ($\pi\alpha$). We will omit them in our investigation.

There are basically two classes of phenomena associated with the presence of intense gauge fields.

Firstly, they can produce pairs of particles. For the Abelian case of strong homogeneous electric field, Sauter [15] showed this by investigating solutions of the Dirac equation in the corresponding potential,[1] and Schwinger [3] by using methods of action integral, Green's functions and proper time. Differential probabilities for pair creation were investigated in Refs. [17] and [18]. In the latter Reference, the quasi–Abelian model was applied to investigation of the quark pair production in chromoelectric flux tubes. Experimental evidence related with the pair production in a strong QED (laser) field was reported in Ref. [19].

The pair production has its origin in the imaginary (absorptive) part of the effective Lagrangian induced by the fermionic quantum fluctuations in the strong field. That part is entirely nonperturbative in nature, because the production effects are $\sim\exp(-\text{const.}/g)$ and thus cannot be expanded in positive powers of the field–to–fermion coupling parameter g.

On the other hand, the other class of phenomena is associated with the real (dispersive) part of the induced effective Lagrangian. In QED, this class includes the following phenomena that affect a low energy ($\omega \ll m_e$) photon wave entering the region of the strong background field: photon splitting, change of the photon speed, and birefringence. Works on the theoretical aspects of these phenomena include Refs. [20]– [24]. The experimental aspects of birefringence in strong magnetic fields are discussed in [25]– [26]. The dispersive part of the induced action leads in principle to those corrections of the classical Maxwell equations which originate from the (fermionic) quantum fluctuations.

The aim of the present paper, while dealing with the dispersive part of the induced action, is somewhat different from these works. We concentrate on the concept of separating the nonperturbative from the perturbative contributions in the induced dispersive action when the product of the (quasi)electric field $\mathcal{E}$ and the coupling constant g is large: $g\mathcal{E}/m^2 \gtrsim 1$, where m is the fermion mass. Subsequently, we numerically investigate the two contributions. Afterwards, we use the discussed quantities as a "laboratory" for testing and investigating the efficiency of methods of quasianalytic continuation. The latter methods, involving the (modified) Borel-Padé approximants, allow us to obtain approximately the nonperturbative contributions from the approximate knowledge of the perturbative contributions and by employing the Cauchy principal value prescription in the inverse Borel transformation (Laplace–Borel integral). These considerations can give us insights into the problems of extraction of nonperturbative physics from the knowledge of perturbative physics in gauge theories, in particular in various versions of QCD (high–flavor, low–flavor).

In Section II, we argue how to perform the mentioned separation into the perturbative

---

[1] A related problem was first considered even earlier by Klein [16] who investigated solutions of the Dirac equation with a high vertical barrier potential (Klein's paradox).

and nonperturbative contributions. After identifying the two contributions, we investigate numerically their values for various values of the field parameter $\tilde{a} \sim g\mathcal{E}/m^2$. In Section III we then carry out an analogous analysis for the induced energy density, the latter being in principle observable. In Section IV we then numerically investigate, for the induced Lagrangian and energy densities, (quasi)analytic continuation from the perturbative into the nonperturbative sectors, employing the method of Borel–Padé for the induced Lagrangian and a modified Borel–Padé for the induced energy density. We encounter integration over renormalon poles, whose origin is nonperturbative, and we show how to carry it out. Section V summarizes our results and conclusions.

II. INDUCED DISPERSIVE LAGRANGIAN DENSITY

We start by considering the Euler–Heisenberg Lagrangian density [1]– [7] which is the part induced by the quantum fluctuations of the fermions in an arbitrarily strong (quasi–)Abelian homogeneous field

$$\delta\mathcal{L} = \frac{1}{8\pi^2}\int_{-\mathrm{i}\epsilon}^{\infty-\mathrm{i}\epsilon}\frac{ds}{s}\exp[-\mathrm{i}s(m^2-\mathrm{i}\varepsilon')]\left[g^2ab\coth(ags)\cot(bgs)-\frac{g^2}{3}(a^2-b^2)-1/s^2\right] . \quad (1)$$

Here, g is the field–to–fermion coupling parameter (in electromagnetism it is the positron charge e_0), m is the mass of the (lightest) fermion, and the parameters a and b are Lorentz–invariant expressions characterizing the (quasi)electric and the (quasi)magnetic fields $\vec{\mathcal{E}}$ and $\vec{\mathcal{B}}$, respectively

$$a = \left[+\vec{\mathcal{E}}^2-\vec{\mathcal{B}}^2+\sqrt{\left(\vec{\mathcal{E}}^2-\vec{\mathcal{B}}^2\right)^2+4\left(\vec{\mathcal{E}}\cdot\vec{\mathcal{B}}\right)^2}\right]^{1/2}/\sqrt{2} , \quad (2)$$

$$b = \left[-\vec{\mathcal{E}}^2+\vec{\mathcal{B}}^2+\sqrt{\left(\vec{\mathcal{E}}^2-\vec{\mathcal{B}}^2\right)^2+4\left(\vec{\mathcal{E}}\cdot\vec{\mathcal{B}}\right)^2}\right]^{1/2}/\sqrt{2} . \quad (3)$$

We note that $ab=|\vec{\mathcal{E}}\cdot\vec{\mathcal{B}}|$, and a^2–$b^2=\vec{\mathcal{E}}^2-\vec{\mathcal{B}}^2$. Further, $a\to|\vec{\mathcal{E}}|$ when $|\vec{\mathcal{B}}|\to 0$, and $b\to|\vec{\mathcal{B}}|$ when $|\vec{\mathcal{E}}|\to 0$. In the Lorentz frame where $\vec{\mathcal{B}}\|\vec{\mathcal{E}}$, we simply have: $a=|\vec{\mathcal{E}}|$ and $b=|\vec{\mathcal{B}}|$. Expression (1) can be obtained, for example, directly by integrating out the fermionic degreees of freedom in the path integral expression of the full effective action, and employing the proper–time integral representation for the difference of logarithms.

As denoted, the integration in (1) is performed along the positive real axis infinitesimally below it, avoiding in this way the poles on the real axis appearing due to the (Lorentz–invariant version of the) magnetic field b (function $\cot(bgs)$ there). If the path in (1) were above the real axis, then we would obtain a nonzero imaginary part of the Lagrangian density even in the pure magnetic field case. This would imply particle creation in this case, which is physically unacceptable. The path in (1) reproduces for the case of the pure magnetic field the known real density, and for the case of the pure electric field the known complex density [3]. The path in (1) is suggested also from the extension of the formal approach of Ref. [7] to the general $ab\neq 0$ case. Namely, when $ab\neq 0$, we need to evaluate in this approach two traces: one trace originating from $a\neq 0$ and discussed in [7] [their Eq. (4-116)]; and the other trace of the evolution operator of an harmonic oscillator, originating from $b\neq 0$ [27], of

the form $\sum \exp[-2\mathrm{i}sgb(n+1/2)]$ ($n=0,1,\ldots$; $s>0$). The latter trace becomes convergent after regularization $s \mapsto s-\mathrm{i}\epsilon$ ($\epsilon \to +0$), i.e., the path in (1).

Performing a contour integration in the fourth quadrant of the complex proper–time s–plane (cf. Fig. 1), expression (1) can be rewritten as

$$\delta\mathcal{L} = -\frac{1}{8\pi^2}\int_{+0}^{\infty}\frac{dz}{(z+\mathrm{i}\epsilon)}\mathrm{e}^{-zm^2}\left[g^2ab\cot\left(ag(z+\mathrm{i}\epsilon)\right)\coth\left(bg(z+\mathrm{i}\epsilon)\right)+\frac{g^2}{3}(a^2-b^2)-\frac{1}{(z+\mathrm{i}\epsilon)^2}\right], \tag{4}$$

where $s=-\mathrm{i}z+\epsilon$ now runs along the negative imaginary axis (and $\epsilon\to+0$). As seen from Fig. 1, the result (4) is actually independent of the precise path of the proper time variable s in (1), as long as s runs from near the origin towards $s=+\infty$ and passes each positive pole on the right, i.e. precisely the class of paths satisfying the physical condition that the pure magnetic fields cannot produce particles. In (1) and (4), the familiar [1] counterterm $\propto(a^2-b^2)$ $[=(\mathcal{E}^2-\mathcal{B}^2)]$ is included which makes the integral finite. This divergent term leads to the renormalization of the field in the leading Lagrangian density $\mathcal{L}^{(0)}=(\mathcal{E}^2-\mathcal{B}^2)/2$. We now divide the integration region into intervals for the integration variable agz: $i_0=[0,\pi/2]$, $i_1=[\pi/2,3\pi/2]$, …, $i_n=[(n-1/2)\pi,(n+1/2)\pi]$, … Each interval, except i_0, contains in its middle one pole of the integrand. The corresponding series for the real (dispersive) part of the Lagrangian density is

$$\mathrm{Re}\delta\tilde{\mathcal{L}} = \mathrm{Re}\delta\tilde{\mathcal{L}}_0+\sum_{n=1}^{\infty}\mathrm{Re}\delta\tilde{\mathcal{L}}_n\ , \tag{5}$$

$$\mathrm{Re}\delta\tilde{\mathcal{L}}_0 = -\int_0^{\pi/2}\frac{dw}{w}\exp\left(-\frac{w}{\tilde{a}}\right)\left[p\cot(w)\coth(pw)+\frac{1}{3}(1-p^2)-\frac{1}{w^2}\right]\ , \tag{6}$$

$$\begin{aligned}\mathrm{Re}\delta\tilde{\mathcal{L}}_n = &-\exp\left(-\frac{n\pi}{\tilde{a}}\right)\left\{\int_{-\pi/2}^{\pi/2}dw\exp\left(-\frac{w}{\tilde{a}}\right)\left[\frac{p\cot(w)\coth(p(w+n\pi))}{(w+n\pi)}\right.\right.\\ &\left.-\frac{p}{w}\frac{\coth(pn\pi)}{n\pi}+\frac{(1-p^2)}{3(w+n\pi)}-\frac{1}{(w+n\pi)^3}\right]\\ &\left.+\mathrm{Re}\int_{-\pi/2}^{\pi/2}dw\exp\left(-\frac{w}{\tilde{a}}\right)\frac{1}{(w+\mathrm{i}\epsilon')}\frac{p\coth(pn\pi)}{n\pi}\right\}\ ,\quad (n\geq 1)\ .\end{aligned} \tag{7}$$

Here, $\epsilon'\equiv\epsilon ga\to+0$, and we used the notation

$$\tilde{a}\equiv\frac{ga}{m^2},\ \tilde{b}\equiv\frac{gb}{m^2},\qquad p\equiv\frac{b}{a}\equiv\frac{\tilde{b}}{\tilde{a}}\ ,\qquad \delta\tilde{\mathcal{L}}\equiv\delta\mathcal{L}/\left(\frac{m^4\tilde{a}^2}{8\pi^2}\right)\ , \tag{8}$$

and we introduced the dimensionless integration variable $w\equiv agz$ when agz is in the interval i_0, and $w\equiv agz-n\pi$ when agz is in the interval i_n ($n\geq 1$). In (7), we separated the integrand into a part that is entirely nonsingular in the integration region, and a part that is singular but gives a finite value of integration since the Cauchy principal ($\mathcal{P}$) value has to be taken. From a formal point of view, we note that $\delta\tilde{\mathcal{L}}_0$ doesn't "feel" the poles of the integrand as depicted in Fig. 1, while $\delta\tilde{\mathcal{L}}_n$ ($n\geq 1$) "feels" the pole $s=-in\pi/(ag)$ via the principal value part in (7) that is proportional to

$$\mathrm{Re}\int_{-\pi/2}^{\pi/2} dw \frac{\exp(-w/\tilde{a})}{(w+\mathrm{i}\epsilon')} \equiv \mathcal{P}\int_{-\pi/2}^{\pi/2}\frac{dw}{w}\exp(-w/\tilde{a}) =$$
$$-\mathrm{E}_1\left(\frac{\pi}{2\tilde{a}}\right) - \mathrm{Ei}\left(\frac{\pi}{2\tilde{a}}\right) = \left\{ \begin{array}{ll} -2\left[x+x^3/(3!\,3)+x^5/(5!\,5)+\cdots\right]|_{x=\pi/(2\tilde{a})} & \text{if } \tilde{a}\gg 1\ , \\ -(e^x/x)\left[1+(1/x)+\cdots\right]|_{x=\pi/(2\tilde{a})} & \text{if } \tilde{a}\ll 1\ . \end{array} \right\} \tag{9}$$

We note that the dispersive part of the induced Lagrangian density as normalized here (5)–(8) depends only on two dimensionless parameters – on parameter $p\equiv b/a$ which characterizes in a Lorentz–invariant manner the ratio of the strengths of the (quasi)electric and (quasi)magnetic fields [cf. (2)–(3)], and on parameter $\tilde{a}\equiv(ga)/m^2$ which characterizes the combined strengths of the (quasi)electric field parameter a and the field–to–fermion coupling g. In the perturbative weak–field limit, $\tilde{a}$ is small. In this case, when reintroducing in (6) $z\equiv w/(ag)$

$$\mathrm{Re}\delta\mathcal{L}_0 = -\frac{1}{8\pi^2}\int_0^{\pi/(2ag)}\frac{dz}{z}\exp(-zm^2)\left[g^2 ab\cot(agz)\coth(bgz)+\frac{g^2}{3}(a^2-b^2)-\frac{1}{z^2}\right], \tag{10}$$

we can see that the real part of expression (4) is approximately reproduced, since formally $\pi/(2ag)\to\infty$. In this case, the conventional perturbative expansion of the dispersive Lagrangian density in powers of g^2 (i.e., inverse powers of x) can be performed (cf. [1], [3])

$$\delta\tilde{\mathcal{L}}^{\mathrm{pert.}} = \left(c_1 1!\,\tilde{a}^2 + c_3 3!\,\tilde{a}^4 + c_5 5!\,\tilde{a}^6 + \cdots\right)\ , \tag{11}$$

where the expansion coefficients are

$$c_1 = \frac{1}{45}\left[(1-p^2)^2+7p^2\right]\ , \quad c_3 = \frac{1}{945}\left[2(1-p^2)^3+13p^2(1-p^2)\right]\ ,$$
$$c_5 = \frac{1}{14175}\left[3(1-p^2)^4+22p^2(1-p^2)^2+19p^4\right]\ ,\ \text{etc.} \tag{12}$$

Expression (11) can be derived alternatively by purely perturbative methods – the terms $\sim\tilde{a}^{2n}$ can be obtained by calculating the one–fermion–loop Feynman diagram with $2n$ photon external legs of zero momenta. Expression (11) is a divergent asymptotic series and it gives the usual perturbative corrections to the Maxwell equations. On the other hand, the formal small–$\tilde{a}$ expansion of $\mathrm{Re}\delta\tilde{\mathcal{L}}_0$ of (6) [or equivalently: (10)] reproduces the terms (11) and yields in addition the terms $\sim\tilde{a}\exp(-\mathrm{const.}/\tilde{a})$. The latter terms may in principle be dangerous for the interpretation of $\mathrm{Re}\delta\tilde{\mathcal{L}}_0$ of (6) as the perturbative part of the induced density, since they are nonanalytic and could thus signal physical nonperturbative effects. However, in the Appendix we demonstrate that these terms are only an artifact of the abruptness of the infrared (IR) proper–time cutoff $z\le 1/\Lambda_{\mathrm{IR}}^2$ ($\Lambda_{\mathrm{IR}}^2=(2/\pi)m^2\tilde{a}\sim m^2\tilde{a}$).[2] These terms are

[2] The energy cutoff $\Lambda_{\mathrm{IR}}\sim m\sqrt{\tilde{a}}$ is low in the case when the perturbative effects dominate (i.e., at $\tilde{a}<1$), but is higher when the nonperturbative effects are significant (at $\tilde{a}>1$). The nonperturbative effects here reside in the infrared (IR) sector of (fermionic) momenta $q<\Lambda_{\mathrm{IR}}$, and the effective contributing size of this sector gets larger when $\tilde{a}$ grows.

therefore not of a physical nonperturbative origin. In the Appendix we further show that $\mathrm{Re}\delta\tilde{\mathcal{L}}_0$ of (6) should be reinterpreted as the limit with an infinitesimally softened IR cutoff, the latter limit being numerically the same but having no nonanalytic terms in the small–$\tilde{a}$ expansion. That expansion is then identical to (11).

On the other hand, the densities $\mathrm{Re}\delta\tilde{\mathcal{L}}_n$ $(n\geq 1)$ of (7) represent the nonperturbative part of the induced dispersive density (5), for two reasons:

- The integration over the proper–time z runs here in the vicinity (in fact, across) the n'th pole of the integrand of (4). The poles of the integrand are in the nonperturbative regions. We recall that these poles are also the source of the nonzero imaginary (absorptive) part of the density leading to the fermion–antifermion pair creation, a clearly nonperturbative phenomenon.

- The densities $\mathrm{Re}\delta\tilde{\mathcal{L}}_n$ $(n\geq 1)$, independently of the pole structure of their integrands, become appreciable only in the strong–field (large–$\tilde{a}$) regime while in the weak–field (small–$\tilde{a}$) regime they decrease faster than any power of $\tilde{a}$, i.e., they do not contribute to the perturbative series (11). Each of the two integrals in the curly brackets of (7) behaves as $\sim\tilde{a}\exp[\pi/(2\tilde{a})]$ when $\tilde{a}\to+0$, and thus the entire $\mathrm{Re}\delta\tilde{\mathcal{L}}_n$ behaves as $\sim\tilde{a}\exp[-(n-1/2)\pi/\tilde{a}]$ $(n\geq 1)$ in this limit.[3]

Therefore, the nonperturbative effects contained in $\mathrm{Re}\delta\tilde{\mathcal{L}}_n$ $(n\geq 1)$ are of two types, one type being characterized by the poles of the integrand, and the other type by what we may call strong–field effects. From the above discussion, it further follows that we have some freedom in choosing the IR proper–time cutoff: $z\leq 1/\Lambda^2_{\mathrm{IR}}$ is such that $\Lambda^2_{\mathrm{IR}}\sim m^2\tilde{a}$ and that all the possible poles must lie at z's above the cutoff $1/\Lambda^2_{\mathrm{IR}}$. We took $\Lambda^2_{\mathrm{IR}}=\kappa m^2\tilde{a}$ with $\kappa=2/\pi$, but any κ satisfying $1/\pi<\kappa\sim 1$ would be acceptable as well.

From a somewhat different perspective, we can imagine transforming a truncated perturbation expansion for $\mathrm{Re}\delta\tilde{\mathcal{L}}^{\mathrm{pert.}}/\tilde{a}$ of (11) (with several terms) via the Borel–Padé approximation. The resulting integrand approximately reproduces the integrand of (4), including the poles structure. Thus the integration over the n'th pole, contained in $\mathrm{Re}\delta\tilde{\mathcal{L}}_n$ of (7), can be interpreted as the n'th renormalon in the density, i.e., a nonperturbative quantity. We will return to this point later in this paper.

Thus, the densities (6) and (7) result in the fermion–induced perturbative and nonperturbative contributions, respectively, to the Maxwell equations. The fields were taken, strictly speaking, to be homogeneous in space and time. In practical terms, this means that they are not allowed to change significantly on the distance and time scales of the Compton wavelength of the fermion $1/m$. For electro–magnetic fields, m is the electron mass, and $1/m$ is about $4\cdot 10^{-13}$ m, and $1.3\cdot 10^{-21}$ s.

An indication of the relative size of the perturbative and nonperturbative fermion–induced corrections to the Maxwell equations can be obtained by comparing the corresponding contributions to the induced Lagrangian density. This is done in Figs. 2-3. Figures 2 (a), (b) show the dimensionless perturbative (6) and nonperturbative (7) induced Lagrangian

---

[3] If we did not take the principal Cauchy value in (7), but some other prescription (which in the case at hand would be wrong), $\mathrm{Re}\delta\tilde{\mathcal{L}}_n$ would behave as $\sim\exp[-n\pi/\tilde{a}]$.

densities, respectively, as functions of the (quasi)electric field parameter $\tilde{a}$ (8), at four different fixed values $p \equiv \tilde{b}/\tilde{a}$ of the magnetic–to–electric field ratio. The case of the pure (quasi)magnetic field (p.m.f.) is also included in the Figures, as function of $\tilde{b}$. For the p.m.f. case, we normalized the Lagrangian density in analogy with (8), i.e., $\delta\tilde{\mathcal{L}}$ is obtained in that case by dividing $\delta\mathcal{L}$ by $m^4\tilde{b}^2/(8\pi^2)$. The separation between the perturbative and the nonperturbative part was performed in the p.m.f. case analogously, i.e., the proper–time $z < \pi/(2bg)$ contributions were defined to be perturbative, and those from $z > \pi/(2bg)$ nonperturbative. We point out, however, that in the latter case the nonperturbative contributions do not involve the renormalon–type ("pole–type") effects, but only strong–field effects (cf. previous discussion). In Fig. 3, the corresponding ratios of the nonperturbative and perturbative induced densities are presented.[4] When moving beyond the perturbative region (i.e., when $\tilde{a} \ll 1$), we see from these Figures that the nonperturbative parts in general become relatively significant and often even dominant.

Once we come into the nonperturbative regime ($\tilde{a} \gtrsim 1$), however, we must keep in mind that the pair creation, originating from the large absorptive part, will become so strong as to render the solutions of the corrected Maxwell equations unstable. We will quantify somewhat this fact in the next Section in the case of the induced energy density in QED.

In Figs. 2 (a), (b), the densities were normalized according to (8), so that the tree–level reference values for the densities are

$$\tilde{\mathcal{L}}^{(0)} \equiv \mathcal{L}^{(0)} / \left(\frac{m^4 \tilde{a}^2}{8\pi^2} \right) = \frac{4\pi^2}{g^2}(1 - p^2) \ . \tag{13}$$

Therefore, increasing only the coupling parameter g, while leaving the (quasi)electric field a unchanged, results in correspondingly larger relative corrections originating from the induced parts, both nonperturbative and perturbative. In the special case of QED, on the other hand, $g = e_0$ is small [$\alpha = e_0^2/(4\pi) \approx 1/137$], and the overall induced Lagrangian density accounts usually for less than 0.5 per mille of the total Lagrangian density when $\tilde{a} \leq 1$ (see the next Section on related points).

III. INDUCED ENERGY DENSITY

In this Section, we discuss the induced energy densities. Energy density is in principle a measurable quantity. It is not Lorentz–invariant. If the (quasi)electric and (quasi)magnetic fields are mutually parallel, the various induced energy densities can be obtained directly from the corresponding induced Lagrangian densities

$$\begin{aligned} & \delta\mathcal{U}_k = a \frac{\partial \mathrm{Re}\delta\mathcal{L}_k}{\partial a}\bigg|_b - \mathrm{Re}\delta\mathcal{L}_k \\ \Rightarrow \quad & \delta\tilde{\mathcal{U}}_k = \tilde{a} \frac{\partial \mathrm{Re}\delta\tilde{\mathcal{L}}_k}{\partial \tilde{a}}\bigg|_{\tilde{b}} + \mathrm{Re}\delta\tilde{\mathcal{L}}_k \quad (k = 0, 1, 2, \ldots) \ , \end{aligned} \tag{14}$$

[4] The total induced dispersive Lagrangian densities, and values of the truncated perturbation series (11) (including $\sim\tilde{a}^8$), are included in Figs. 6 in Section IV.

where we denoted, in analogy with (8)

$$\delta\tilde{\mathcal{U}}_{(k)} \equiv \delta\mathcal{U}_{(k)} / \left(\frac{m^4\tilde{a}^2}{8\pi^2}\right) \ . \tag{15}$$

With the restriction to parallel fields $\vec{\mathcal{E}} \parallel \vec{\mathcal{B}}$ (i.e, $|\vec{\mathcal{E}}| = a$ and $|\vec{\mathcal{B}}| = b$) we do not lose the generality since, for any configuration of $\vec{\mathcal{E}}$ and $\vec{\mathcal{B}}$, there always exists a Lorentz boost, perpendicular to the plane of the fields, so that in the boosted frame the two fields are parallel. The corresponding perturbative and nonperturbative parts of the energy densities in such frames are

$$\begin{aligned}
\mathrm{Re}\delta\tilde{\mathcal{U}}_0 = & -\int_0^{\pi/2} \frac{dw}{w} \exp\left(-\frac{w}{\tilde{a}}\right) \Bigg\{ \left(\frac{w}{\tilde{a}} - 1\right) \left[p\cot(w)\coth(pw) + \frac{1}{3}(1-p^2) - \frac{1}{w^2}\right] \\
& + \left[p\cot(w)\coth(pw) + p^2 \frac{w\cot(w)}{\sinh^2(pw)} + \frac{2}{3} - \frac{2}{w^2}\right] \Bigg\} \ , \qquad (16) \\
\mathrm{Re}\delta\tilde{\mathcal{U}}_n = & -\exp\left(-\frac{n\pi}{\tilde{a}}\right) \Bigg\{ \int_{-\pi/2}^{\pi/2} dw \exp\left(-\frac{w}{\tilde{a}}\right) \left[\frac{(w+n\pi)}{\tilde{a}} - 1\right] \left[\frac{p\cot(w)\coth(p(w+n\pi))}{(w+n\pi)}\right. \\
& \left. -\frac{p}{w}\frac{\coth(pn\pi)}{n\pi} + \frac{(1-p^2)}{3(w+n\pi)} - \frac{1}{(w+n\pi)^3}\right] \\
& + \int_{-\pi/2}^{\pi/2} dw \exp\left(-\frac{w}{\tilde{a}}\right) \left[p\cot(w)\left(\frac{\coth(p(w+n\pi))}{(w+n\pi)} + \frac{p}{\sinh^2(p(w+n\pi))}\right)\right. \\
& \left. -\frac{p}{w}\left(\frac{\coth(pn\pi)}{n\pi} + \frac{p}{\sinh^2(pn\pi)}\right) + \frac{2}{3}\frac{1}{(w+n\pi)} - \frac{2}{(w+n\pi)^3}\right] \\
& + \left[\frac{p}{\tilde{a}}\coth(pn\pi) + \frac{p^2}{\sinh^2(pn\pi)}\right] \left[-\mathrm{E}_1\left(\frac{\pi}{2\tilde{a}}\right) - \mathrm{Ei}\left(\frac{\pi}{2\tilde{a}}\right)\right] \\
& + \frac{2p}{n\pi}\coth(pn\pi)\sinh\left(\frac{\pi}{2\tilde{a}}\right) \Bigg\} \ , \quad (n \geq 1) \ . \qquad (17)
\end{aligned}$$

The tree–level density in the normalization convention used [cf. (8)] is

$$\tilde{\mathcal{U}}^{(0)} \equiv \mathcal{U}^{(0)} / \left(\frac{m^4\tilde{a}^2}{8\pi^2}\right) = \frac{4\pi^2}{g^2}(1+p^2) \ . \tag{18}$$

The perturbative power expansion of the induced energy density $\delta\tilde{\mathcal{U}}$ is

$$\delta\tilde{\mathcal{U}}^{\mathrm{pert.}} = \left(d_1 1!\,\tilde{a}^2 + d_3 3!\,\tilde{a}^4 + d_5 5!\,\tilde{a}^6 + \cdots\right) \ , \tag{19}$$

where the expansion coefficients are

$$\begin{aligned}
& d_1 = \frac{1}{45}\left[3 + 5p^2 - p^4\right] \ , \quad d_3 = \frac{1}{945}\left[10 + 21p^2 - 7p^4 + 2p^6\right] \ , \\
& d_5 = \frac{1}{14175}\left[21 + 50p^2 - 21p^4 + 10p^6 - 3p^8\right] \ , \ \text{etc.} \qquad (20)
\end{aligned}$$

The results for the induced perturbative (16) and nonperturbative parts (17), and their ratios, are presented in Figs. 4 (a)–(b) and 5, respectively, in analogy with Figs. 2 (a)–(b)

and 3. The case of the pure (quasi)magnetic field is not included in Figs. 4–5, because in this case $\delta\tilde{\mathcal{U}} = -\delta\tilde{\mathcal{L}}$ and thus the relevant information is already contained in Figs. 2–3. The behavior of the induced energy densities is, in broad qualitative terms, similar to that of the induced Lagrangian densities.[5]

In the special case of QED, similarly as for the Lagrangian densities in the previous Section, the total induced energy densities account for a very small part of the total energy density (0.2–0.3 per mille when $\tilde{a} \approx 1$) and can become significant only when the field becomes exceedingly large ($\tilde{a} \gtrsim 10^2$). The same is true also for the dielectric permeability tensor ε_{ij}: In the direction of the fields, we have $\delta\varepsilon_{\parallel} \equiv \varepsilon_{\parallel} - 1 = a\partial(\mathrm{Re}\delta\mathcal{L})/\partial a|_b$, i.e., by (14)–(15) we have $\delta\varepsilon_{\parallel} = (\delta\tilde{\mathcal{U}} + \mathrm{Re}\delta\tilde{\mathcal{L}})\alpha/(2\pi)$, which is about 10^{-3} for $\tilde{a} \approx 1$ and $p = 1$. Therefore, the effective coupling parameter along the field direction $\alpha_{\parallel} = \alpha/\varepsilon_{\parallel}$ changes by about one per mille, while $\alpha_{\perp} = \alpha/\varepsilon_{\perp}$ remains unchanged since $\varepsilon_{\perp} = 1$. Therefore, in QED, any quantity which can be expanded in powers of the coupling parameter alone (without fields) remains a perturbative quantity. QED then remains a perturbative theory despite such strong fields – cf. also Ref. [28] on that point.

The energy density is not stable in time when $\tilde{a} \neq 0$, due to the energy losses to pair creation of fermions of mass m. It decreases by about 50 percent in the time $t_{1/2}$

$$t_{1/2} \approx \frac{\pi^2}{8\alpha} \exp\left(+\frac{\pi}{\tilde{a}}\right) \left[\frac{(1+p^2)}{p\pi \coth(p\pi)}\right] \frac{1}{m} \,, \tag{21}$$

where $\alpha \equiv g^2/(4\pi)$. The factor in the square brackets, appearing due to the presence of the (quasi)magnetic field, is usually not essential in the estimates since it is ~ 1 for $p \leq 5$. In the case of QED and with $p = 0$, $t_{1/2}$ is about $0.9 \cdot 10^5 m_e^{-1}$, $0.4 \cdot 10^4 m_e^{-1}$ and $0.3 \cdot 10^3 m_e^{-1}$ for $\tilde{a} = 0.5$, 1, and 5, respectively. Here, $m_e^{-1} \approx 1.3 \cdot 10^{-21}$ s is the electron Compton time.

IV. QUASIANALYTIC CONTINUATION INTO THE NONPERTURBATIVE SECTOR

In this Section, we use the discussed induced densities as an example on which to test and get some insights into methods of approximate analytic (i.e., quasianalytic) continuation. In various physical contexts, such methods allow one to extract all or part of the information on the nonperturbative sector from the knowledge of the perturbative sector alone. We will use the method of Borel–Padé transformation, or a modification thereof.

One may ask whether the perturbation expansions (11) and (19) allow us to obtain the full, including the nonperturbative, information about the corresponding densities. The answer for the Lagrangian density is yes, but under the condition that we take in the corresponding Borel–Padé approximants the Cauchy principal values when integrating over the positive poles of the Padé integrand in the inverse Borel transformation. This is reflected in the terms $i\epsilon$ in the denominators of the integrands of (4) and/or (7). More specifically, we first Borel–transform (B) the perturbation series (11)

---

[5] The total induced energy densities, and values of the truncated perturbation series (19) that include terms $\sim \tilde{a}^8$, are included in Figs. 7 in Section IV.

$$B\left[\frac{\delta\tilde{\mathcal{L}}^{\rm pert.}(\tilde{a};p)}{\tilde{a}}\right]=c_1(p)\tilde{a}+c_3(p)\tilde{a}^3+c_5(p)\tilde{a}^5+\cdots\ , \tag{22}$$

then construct an $[N/M]_{\rm B}(\tilde{a};p)$ Padé approximant to B of (22),[6] and then apply the inverse Borel transformation

$$BP^{[{\rm N/M}]}\left[\delta\tilde{\mathcal{L}}^{\rm pert.}\right](\tilde{a};p)=\int_0^\infty dw\exp\left(-\frac{w}{\tilde{a}}\right)[N/M]_{\rm B}(w;p)\ . \tag{23}$$

On the other hand, the real part of the actual density (4) can also be written as a Borel–type integral, when introducing $w\equiv agz$ and $\epsilon'\equiv ag\epsilon$ in (4) and normalizing the density according to (8)

$${\rm Re}\delta\tilde{\mathcal{L}}={\rm Re}\int_0^\infty dw\exp\left(-\frac{w}{\tilde{a}}\right)\frac{(-1)}{w}\left[\frac{p\cos(w)}{\sin(w+{\rm i}\epsilon')}\coth(pw)+\frac{1}{3}(1-p^2)-\frac{1}{w^2}\right]\ . \tag{24}$$

The expansion of the integrand of (24), excluding the exponential, in powers of w is identical with the Borel transform (22) with $\tilde{a}\mapsto w$, as it should be. Comparing (23) with the exact result (24), we see that the Borel–Padé method (23) will be efficient in (quasi)analytic continuation if Padé approximants $[N/M]_{\rm B}(w)$ approach the integrand of (24) in an increasingly wide integration interval of w when the Padé order indices N and M ($\approx N$) increase. This in fact happens, since the integrand in (24) is a meromorphic function in the complex plane whose poles structure on the positive axis is especially simple – there are only single (not multiple) poles, located at $w=\pi,2\pi,3\pi$. Padé approximants to power expansions of such functions are known to approximate such functions increasingly better when the Padé order indices $N\approx M$ increase [29]. Near the poles $w\approx n\pi$ the integrand behaves as $\sim(w-n\pi+{\rm i}\epsilon')^{-1}$. Hence, for obtaining the real (dispersive) part of the density, the Borel integration over the poles has to be taken with the Cauchy principal value (CPV) prescription – not just in the exact expression (24), but also in the approximate expression (23). Thus, the Borel integration in (23) over the n'th pole, i.e., the n'th renormalon contribution, has in the case at hand no renormalon ambiguity. As the Padé order indices $N\approx M$ are increased, we thus systematically approach the exact ${\rm Re}\delta\tilde{\mathcal{L}}$ via the CPV of (23). This means that in the case at hand [strong (quasi–)Abelian fields with fermionic fluctuations included], the full induced Lagrangian density can be obtained on the basis of the knowledge of perturbation expansion (11) for weak fields and the CPV prescription. The more terms in (11) [and thus in (22)] we know, the higher Padé order indices $N\approx M$ we can have, and hence the closer to the full Lagrangian density we can come via (23).

On the basis of the knowledge of the first four nonzero perturbation terms in (11) and correspondingly in (22), we can construct the following Padé approximants of the perturbative Borel transform (22): $[1/2]_{\rm B},[1/4]_{\rm B},[3/4]_{\rm B}$. Then we can calculate the corresponding

---

[6] $[N/M](\tilde{a})$ Padé approximant to (22) is defined by two properties: 1. it is a ratio of two polynomials in $\tilde{a}$, the nominator polynomial having the highest power $\tilde{a}^N$ and the denominator $\tilde{a}^M$; 2. when expanded in powers of $\tilde{a}$, it reproduces the coefficients at the terms $\tilde{a}^n$ in (22) for $n\leq N+M$; it is based solely on the knowledge of these latter coefficients c_n ($n\leq N+M$).

Borel-Padé transforms via (23) with the CPV prescription. The corresponding results of the approximants for the full induced density $\mathrm{Re}\delta\tilde{\mathcal{L}}$ are presented in Fig. 6, together with the exact numerical values calculated by (24) in Section II. The curves are given as functions of the (quasi)electric strength parameter $\tilde{a}$ for four fixed values of the magnetic–to–electric field ratio p, and Fig. 6 (d) is for the case of the pure (quasi)magnetic field ($\tilde{a}=0$). We see that the highest order ([3/4]) Padé–Borel results agree well with the exact results over the entire depicted region of $\tilde{a}$. When the Padé order indices N and M ($\sim N$) increase, the region of agreement includes increasingly large values of $\tilde{a}$. For comparison, we also included the results of the truncated perturbation series (TPS) made up of the first four nonzero terms of (11) [in Fig. (d): for the corresponding p.m.f. case], i.e., those perturbation terms which the presented Borel–Padé transforms are based on.

If we apply the very same procedure in the case of the energy density – Borel–transforming the series $\delta\tilde{\mathcal{U}}^{\mathrm{pert.}}/\tilde{a}$ of (19), constructing Padé approximants, and carrying out the inverse Borel transformation by using the Cauchy principal value (CPV) prescription – the results are disappointing. It turns out that increasing the Padé order indices N and M ($\sim N$) does not generally result in a better precision. For example, for $p \overset{<}{\approx} 0.5$ and $\tilde{a} \overset{>}{\approx} 0.5$, the Borel–Padé transforms of the order [3/4] and [3/6] give significantly worse results than those of the lower order [1/4]. The reason for this erratic behavior of the Borel–Padé approximants in this case lies in the more complicated poles structure of the Borel–Padé transforms. This can be seen if we rewrite $\delta\tilde{\mathcal{U}}$ in the Borel–integral form analogous to (24), obtained from (24) by applying relation (14)

$$\mathrm{Re}\delta\tilde{\mathcal{U}} = \mathrm{Re}\int_0^\infty dw \exp\left(-\frac{w}{\tilde{a}}\right)\frac{(-1)}{w}\left[-\frac{pw}{\sin^2(w+\mathrm{i}\epsilon')}\coth(pw)+\frac{1}{3}(1+p^2)+\frac{1}{w^2}\right] . \qquad (25)$$

The expansion in powers of w of the integrand in (25), excluding the exponential, gives of course the exact Borel transform of the perturbation series (19) divided by $\tilde{a}$ (and replacing $\tilde{a}\mapsto w$)

$$\begin{aligned} &-\frac{1}{w}\left[-\frac{pw}{\sin^2(w+\mathrm{i}\epsilon')}\coth(pw)+\frac{1}{3}(1-p^2)+\frac{1}{w^2}\right] \\ &= d_1(p)w + d_3(p)w^3 + d_5(p)w^5 + \cdots \equiv B\left[\frac{\delta\tilde{\mathcal{U}}^{\mathrm{pert.}}(w;p)}{w}\right] . \end{aligned} \qquad (26)$$

However, we now see that this integrand has a double poles structure on the positive w axis, the double poles located at $w=\pi, 2\pi, 3\pi, \ldots$. The Padé approximants to the power series (26) have great trouble simulating this double poles structure adequately. When they do it by creating one single or two nearby real poles, say near $w=\pi$, then it turns out that the inverse Borel transformation via the Cauchy principal value (CPV) prescription often gives good results. However, when the Padé approximants try to simulate the double pole near $w=\pi$ by creating two mutually complex–conjugate poles $a\pm\mathrm{i}b$ ($a\approx\pi$, $|b|\ll\pi$), the inverse Borel transformation gives very unsatisfactory results. This occurs, for example, in Padé approximants $[3/4](w;p)$ and $[3/6](w;p)$ for $p\leq 0.5$. Heuristically we can understand that such a simulation is bad, because the structure of the integrand in (25) suggests that a double pole at a–ib alone, just below the real axis, would do a better job, but it is not allowed in the Padé approximants. The latter is true because the perturbation expansion (26) is

explicitly real for real w's, and this property is hence shared also by the Padé approximants, enforcing for each complex pole another pole which is complex–conjugate.

To overcome this problem, the idea is to modify the Borel transformation of the perturbation series (19) in such a way that the resulting transformed series is represented by a (meromorphic) function without any double poles on the real positive axis, in contrast to the Borel–transformed series (26). This, in fact, can be implemented in the easiest way by using the following modification of the Borel transformation (MB):

$$\frac{\partial MB\left[\delta\tilde{\mathcal{U}}^{\rm pert.}\right](w;p)}{\partial w} = B\left[\frac{\delta\tilde{\mathcal{U}}^{\rm pert.}(w;p)}{w}\right] = d_1(p)w + d_3(p)w^3 + d_5(p)w^5 + \cdots$$

$$\Rightarrow \quad MB\left[\delta\tilde{\mathcal{U}}^{\rm pert.}\right](w;p) = d_1(p)\frac{w^2}{2} + d_3(p)\frac{w^4}{4} + d_5(p)\frac{w^6}{6} + \cdots \ . \tag{27}$$

This trick changes every double pole in the B into the corresponding single pole in the MB. Then we apply Padé approximants $[N/M]_{\rm MB}(w)$ to the MB series (27), and carry out the corresponding inverse modified Borel transformation

$$MBP^{[{\rm N/M}]}\left[\delta\tilde{\mathcal{U}}^{\rm pert.}\right](\tilde{a};p) = \frac{1}{\tilde{a}}\int_0^\infty dw \exp\left(-\frac{w}{\tilde{a}}\right)[N/M]_{\rm MB}(w;p) \tag{28}$$

with the Cauchy principal value (CPV) prescription when integrating over the single poles. This CPV prescription originates again from the $\mathrm{i}\epsilon'$ terms in the double poles structure $(w-n\pi+\mathrm{i}\epsilon')^{-2}$ of the Borel–transform (B) integrand of (25) that is now changed to the single poles structure $(w-n\pi+\mathrm{i}\epsilon')^{-1}$ in the modified Borel–transform (MB) of (27) whose Padé approximants $[N/M]_{\rm MB}(w;p)$ appear in (28).

The numerics clearly confirm that these MBP's (28) are well behaved, i.e., they approximate well the actual full induced energy density $\delta\tilde{\mathcal{U}}(\tilde{a};p)$ in the region of $\tilde{a}$ which is getting wider when the Padé order indices N and M ($\approx N$) increase. The results are presented in Fig. 7, where the MBP's for the first three possible Padé order indices [2/2], [2/4] and [4/4], along with the exact numerical results, are shown as functions of $\tilde{a}$, at four fixed values of $p \equiv \tilde{b}/\tilde{a}$. Another reason why the results now behave better than those of the usual BP tranforms lies in the fact that the Padé approximants ([2/2], [2/4] and [4/4]) are now more diagonal than earlier ([1/2], [1/4] and [3/4]). This is due to one additional power of w in the MB series (27), as compared with the usual B series. The diagonal and near–diagonal Padé approximants are known to behave better than the (far) off–diagonal ones [29]. In fact, Figs. 7 suggest that clear improvement – extension of the $\tilde{a}$ range of agreement with the exact results – sets in when we switch from [2/2] to [4/4] MBP, while the off–diagonal [2/4] MBP may even be slightly worse than [2/2]. For comparison, we also included the results of the truncated perturbation series (TPS) made up of the first four nonzero terms (up to $\sim\tilde{a}^8$) of (19), i.e., the terms on which the presented Borel–Padé transforms are based. The case of the pure (quasi)magnetic field was not included in these Figures because in this case $\delta\tilde{\mathcal{U}} = -\delta\tilde{\mathcal{L}}$ and thus the information on this case is contained in Fig. 6 (d).

This application of Borel–Padé transformations and their modification may give us some insights into how the (quasi)analytic continuation from the perturbative (small $\tilde{a}$) into the nonperturbative (large $\tilde{a}$) regions can be carried out in other theories whose exact behavior in the latter region is still theoretically unknown. One such example is the perturbative QCD (pQCD), where some observables are known at the next–to–next–to–leading order ($\mathrm{N^2LO}$).

The coupling parameter in that case [$\tilde{a} \mapsto \alpha_s(Q^2)$] can be quite large when the relevant energies of the process are low ($Q \sim 1$ GeV), thus rendering the direct evaluation of the N^{2}LO TPS unreasonable or at best unreliable. When applying Borel–Padé transformations or modifications thereof to such series, we are faced with two major problems:

- The first problem is of a more technical nature. Since only very few, at most two, coefficients beyond the leading order are known, the Padé approximants associated with the (modified) Borel transform of the series have low order indices ($N, M \leq 2$) and thus do not necessarily reproduce the location of the leading poles on the positive axis, if they exist, adequately.

- The second problem is of a deeper theoretical nature. Knowing too little about the behavior of QCD in, or close to, the nonperturbative regime, we do not know how to integrate over the possible positive poles in the inverse (modified) Borel transformation – this can be termed the infrared renormalon ambiguity [30].

In the discussed case of integrated fermionic fluctuations in strong (quasi–)Abelian fields – for the Lagrangian and energy densities – we do not face any of the two afore–mentioned problems since the exact solution is known. We have to apply the Cauchy principal value (CPV) prescription in the integration of the Borel–Padé transform of the induced dispersive Lagrangian density, and in the modified Borel–Padé transform of the induced energy density. The CPV is the direct consequence of the path (ϵ parameter) in the exact solution (1) [$\Leftrightarrow$ (4)]. The knowledge of the full theoretical solution in the latter case also tells us that the poles structure of the usual Borel transform of the induced energy density is more complicated (double poles), so that we have to apply a modified Borel-Padé transform which changes the double poles into a single poles structure.

We point out that the positive poles – renormalons – discussed in the present work cannot be directly identified with the usual infrared (ultraviolet) renormalons in QCD (QED). The latter renormalons, as defined in the literature [30], are interpreted in the perturbative language as originating from renormalon chains at low (high) momenta k. The renormalon chains are momentum–k gluon (photon) propagators with n chained one–loop insertions, where n can be arbitrarily large. In the model at hand, however, only quantum fluctuations of fermions, in the slowly–varying strong fields, are considered; the effects of the quantum fluctuations of propagating gluons (photons) were not included in the discussed effective model. The positive poles, i.e. renormalons, in the present model originate from a collective effect of arbitrarily many very soft gluons (photons) coupling to a fermion loop or to a fermion propagator – cf. [31]. The relevant parameter of the effective coupling of these soft gauge bosons to the fermions, appearing in the induced effective action, is $\tilde{a} = ga/m^2$ and it can be large due to the strong field a and/or due to the strong coupling g. These nonperturbative contributions are then roughly $\sim \exp(-\text{const.}/\tilde{a}) = \exp[-\text{const.}m^2/(ga)]$ – cf. (23), (28). This is similar, but not identical, to the infrared renormalon contributions in QCD $\sim \exp(-\text{const.}'/g^2)$. We may be tempted to term the renormalons discussed in the present paper as infrared renormalons due to their nonperturbative origin in the infrared, although this name is reserved for the afore–mentioned QCD–type renormalons.

Various QCD and QED applications of the Borel-Padé approach, with CPV prescription, have been made in [32]– [34]. The new method of Ref. [34] gives modified real and imaginary parts of the Borel–Padé of $\delta\tilde{\mathcal{L}}$, in comparison to the usual CPV prescription, when the Padé

approximants $[N/M]_B$ have poles off the positive real axis. This may influence the speed of the convergence of the Borel–Padé transforms towards the full solution when the Padé order indices N and M ($\approx N$) increase. This method came to our attention after finishing the manuscript.

Two other references [35]– [36] are also somewhat related to our work. Dunne and Hall [35] considered, among other things, the question of resummation of the (one–loop) Euler–Heisenberg (EH) Lagrangian density by using the knowledge of the perturbation expansion of the Borel transform. Since they did not use Padé in addition, they needed at least an approximate information on *all* the coefficients of the series to reconstruct approximately the nonperturbative sector. Jentschura *et al.* [36], on the other hand, did not employ the Borel transform, but applied directly to truncated perturbation series (TPS) of the EH density a numerical method (Weniger sequence transformation) which differs from Padé in several aspects. Their results of resummation are better than the direct application of Padé to the TPS of the EH Lagrangian, but they are worse than the results of the combined Borel–Padé method.

V. CONCLUSIONS

We introduced the concept of separation of the induced dispersive action into the nonperturbative and perturbative parts. We then investigated numerically the nonperturbative contributions to the dispersive (real) part of the Lagrangian density and to the real energy density, induced by quantum fluctuations of fermions in the strong (quasi–)Abelian fields that don't change significantly in space–time over the typical fermionic Compton wavelengths $1/m$. There are only nonperturbative contributions in the absorptive (imaginary) part of the strong field Lagrangian density, the latter part being responsible for the fermion–antifermion pair creation. On the other hand, the nonperturbative contributions in the real (dispersive) sector are in general also significant and can often even dominate over the perturbative induced contributions there. The induced dispersive Lagrangian density modifies the Maxwell equations for strong fields. The induced energy density is in principle an observable quantity. When the (quasi)electric fields are strong, however, these densities decay fast (in $\sim 10^3$ Compton times, for $\tilde{a} \sim 1$). These two induced densities lead to a change in the dielectric permeability tensor of the vacuum. In the special case of QED, all these induced effects are below one per cent unless the fields are huge ($\tilde{a} \sim 10^2$).

We then used the discussed induced quantities as a "laboratory" to test and investigate the efficiency of specific methods of quasianalytic continuation from the perturbative region (weak fields) into the nonperturbative region (strong fields). We employed the method of Borel–Padé for the induced dispersive Lagrangian density, since the function represented by the Borel transform series has only simple poles. For the induced energy density, we had to employ a modified Borel–Padé transformation since the function represented by the (nonmodified) Borel transform series has double poles. We found out numerically that such quasianalytic continuations become precise over an increasing region of the effective expansion parameter $\tilde{a}$ when the number of available terms in the perturbative expansion increases. This means that the quasianalytic continuation gradually becomes the analytic (exact) continuation when the number of the perturbative expansion terms accounted for increases. The Borel integration over positive poles (renormalons) is necessary. The correct

prescription for the integration over these poles, in the case at hand, is the simplest one – the Cauchy principal value (CPV) prescription, its origin being the path (ϵ parameter) in the exact solution (1) [$\Leftrightarrow$ (4)]. Such analyses could give us some insight into the problems faced in QCD when nonperturbative contributions to observables are investigated either on the basis of the perturbative results themselves or by using other models [37] that are at least partly motivated by perturbative methods.

The correct analytic continuation, in the discussed case of strong background gauge fields, is the one employing the simplest (CPV) prescription for integration over the poles in the Laplace–Borel integral. This appears to be in agreement with the conclusions of Ref. [38] which were obtained from quite different considerations involving the renormalization group – that the vacuum polarization induced by the intense gauge fields is in principle determined by the information on the behavior of the theory in the perturbative region. The situation in QCD is less clear. A necessary condition for the existence of the (correct) analytic continuation from the perturbative into the nonperturbative regime in QCD is that a nontrivial infrared stable fixed point exist for the running strong coupling parameter. Such an infrared stable fixed point, however, seems to exist only if the number of the quark flavors is high ($N_f > 9$) [39]. For the real (low–N_f) QCD, a phase transition takes place, and methods of analytic continuation have probably only a limited range of applicability. Stated differently, in this case the full knowledge of the perturbative sector probably does not allow us to obtain information on the deep nonperturbative sector. In such a case, it is probable that even the renormalon ambiguity in the low–flavor perturbative QCD (pQCD) is an intrinsic ambiguity that cannot be entirely eliminated with pQCD–related methods alone.

ACKNOWLEDGMENTS

The work of G.C. was supported by the Korean Science and Engineering Foundation (KOSEF). The work of J.-Y.Y. was supported by the German Federal Ministry of Science (BMBF).

Appendix A. ON THE ANALYTICITY OF $\delta\tilde{\mathcal{L}}_0$

In this Appendix we will clarify the nature of the nonanalytic terms $\sim\exp(-\text{const.}/\tilde{a})$ that appear in the naive expansion of the perturbative part $\text{Re}\delta\tilde{\mathcal{L}}_0(\tilde{a};p)$ of (6) around the point $\tilde{a}=0$. Such terms may in principle be dangerous for our interpretation of (6) as the perturbative part of the induced Lagrangian density, because they have the nonanalytic structure similar to those terms that appear in the nonperturbative parts $\text{Re}\delta\tilde{\mathcal{L}}_n(\tilde{a};p)$ of (7), the latter containing genuinely nonperturbative contributions due to the singular (pole) structure of the integrand. We will show that the mentioned terms in (6) are an artifact of having the abrupt infrared (IR) cutoff there, and that they disappear as soon as the abruptness of the infrared cutoff is (infinitesimally) softened.

In the proper–time formalism, the IR and UV regions correspond to the high and the low values of the proper time, respectively [40]. In the proper–time integral (4) for $\delta\mathcal{L}$, the IR region of large proper time z [$z \geq \pi/(ag)$] contains poles, the latter leading to nonperturbative effects. The region of smaller z has no such singularities and thus no

nonperturbative effects. Therefore, the perturbative part of $\delta\mathcal{L}$ should cover the latter region, and suppress the IR region. The general way to do this is to introduce, in the spirit of approaches of [40], a nonnegative regulator $\rho_\varepsilon(w)$ ($w\equiv agz$) in the proper–time integral

$$\mathrm{Re}\delta\tilde{\mathcal{L}}^{(\mathrm{P.})}_\varepsilon = -\mathrm{Re}\int_0^\infty \frac{dw}{w}\rho_\varepsilon(w)\exp\left(-\frac{w}{\tilde{a}}\right)\left[p\cot(w+\mathrm{i}\epsilon')\coth(pw)+\frac{1}{3}(1-p^2)-\frac{1}{w^2}\right]\ , \quad \text{(A.1)}$$

where the minimal IR regularization requirements are

$$\rho_\varepsilon(w)\approx 1 \quad \text{for } w\ll 1\ , \qquad \rho_\varepsilon(w)\ll 1 \quad \text{for } w\stackrel{>}{\approx}\pi\ . \quad \text{(A.2)}$$

The nonnegative parameter ε indicates that we can choose a class of such regulators. In fact, we will require that for small ε a large chunk of the perturbative region, namely the w–region of approximately $[0,\pi/2]$, survive in (A.1). Thus we restrict the minimal conditions (A.2) to the following ones, when $\varepsilon\ll 1$:

$$\rho_\varepsilon(w)\approx 1 \quad \text{for } w\stackrel{<}{\approx}\pi/2-\sqrt{\varepsilon}\ , \qquad \rho_\varepsilon(w)\ll 1 \quad \text{for } w\stackrel{>}{\approx}\pi/2+\sqrt{\varepsilon}\ . \quad \text{(A.3)}$$

A seeming alternative to (A.1) would be to introduce a regulator $\rho_\varepsilon(z)$ that would scale as a function of $z\equiv w/(ag)$ instead of w. But this possibility must be discarded because then the condition of suppressing the pole structure [$\rho_\varepsilon(z)\ll 1$ for $z\geq\pi/(ga)\equiv\pi/(m^2\tilde{a})$] cannot be reconciled with the condition of the survival of a large chunk of the perturbative region [$\rho_\varepsilon(z)\approx 1$ for $z\leq\pi/(2m^2\tilde{a})$] at various values of $\tilde{a}$ simultaneously.

The conditions (A.3) are designed in such a way that the limit $\varepsilon\to+0$ would apparently lead to the abrupt IR regulator appearing in $\mathrm{Re}\delta\tilde{\mathcal{L}}_0(\tilde{a};p)$ of (6), with the abrupt cutoff at $w=\pi/2$. We can choose the following specific one–parameter family of regulators $\rho_\varepsilon(w)$ satisfying the afore–mentioned conditions:

$$\rho_\varepsilon(w)=\frac{\tilde{\rho}_\varepsilon(w)}{\tilde{\rho}_\varepsilon(0)}\ , \quad \tilde{\rho}_\varepsilon(w)=\frac{1}{2}-\frac{1}{\pi}\arctan\left(\frac{w-\pi/2}{\varepsilon}\right)\ . \quad \text{(A.4)}$$

When $\varepsilon\to+0$ ($\varepsilon\neq 0$), these regulators differ from the abrupt cutoff regulator outside the narrow w–interval $[\pi/2-\sqrt{\varepsilon},\pi/2+\sqrt{\varepsilon}]$ by at most $\sim\sqrt{\varepsilon}$

$$\rho_\varepsilon(w)=\left\{\begin{array}{ll} 1-(\varepsilon/\pi)(\pi/2-w)^{-1}+\mathcal{O}(\varepsilon^2) & \text{if } w<\frac{\pi}{2}-\sqrt{\varepsilon}\ , \\ (\varepsilon/\pi)(w-\pi/2)^{-1}+\mathcal{O}(\varepsilon^2) & \text{if } w>\frac{\pi}{2}+\sqrt{\varepsilon}\ , \end{array}\right\} \quad \text{(A.5)}$$

while they may differ from the abrupt version significantly only in the afore–mentioned narrow interval. The first thing to check would be that the regularized expression (A.1) with the regulator (A.4)–(A.5), in the limit $\varepsilon\to+0$ ($\varepsilon\neq 0$) really gives numerically the result (6) of the abrupt cutoff. Stated otherwise, we should check that the $\lim_{\varepsilon\to+0}$ in front of the integral (A.1) can be moved into the integral, without changing the result. For such a check, we need to see that the contributions in (A.1) from the singular (poles) regions ($w>\pi/2$) are suppressed toward zero when $\varepsilon\to+0$. Such a check is straightforward and we performed it. It turns out that the w–regions $[(n-1/2)\pi,(n+1/2)\pi]$ around the n'th pole $w_n=n\pi$ are suppressed by a factor $\sim\varepsilon$ when $n\geq 2$, and by at least a factor $\sim\sqrt{\varepsilon}$ when $n=1$. Thus, all these contributions go to zero when $\varepsilon\to+0$. On the other hand, on the w–interval $[0,\pi/2]$, there are no singularities of the integrand and the regulator is virtually equal to 1 in the

entire interval when $\varepsilon \to +0$. Therefore, on this interval we can automatically push the limiting procedure into the integral. Thus we really have

$$\lim_{\varepsilon \to +0} \mathrm{Re}\delta\tilde{\mathcal{L}}_{\varepsilon}^{(\mathrm{P.})}(\tilde{a};p) = \mathrm{Re}\delta\tilde{\mathcal{L}}_{0}(\tilde{a};p) \ , \tag{A.6}$$

i.e., the numerical value of the perturbative part with the infinitesimally "softened" IR cutoff is the same as that of the perturbative part with the abrupt IR cutoff (6).

Now we will investigate the expansions of the above two expressions around the point $\tilde{a}=0$, in order to see the difference in the (non)analiticity structure between the two cases. We can find the small–$\tilde{a}$ expansion of $\mathrm{Re}\delta\tilde{\mathcal{L}}_0(\tilde{a};p)$ of (6) by expanding first the integrand (without the exponent) there, i.e., the Borel transform, in powers of w. As argued in Section IV [cf. Eqs. (22)–(24)], this expansion yields (22) with $\tilde{a} \mapsto w$, where $c_j(p)$'s are given by (12). Then the term–by–term integration over w leads to the small–$\tilde{a}$ expansion of $\mathrm{Re}\delta\tilde{\mathcal{L}}_0$

$$\begin{aligned}
\mathrm{Re}\delta\tilde{\mathcal{L}}_0(\tilde{a};p)^{(\mathrm{exp.})} &= c_1(p)\int_0^{\pi/2} dw \exp(-w/\tilde{a})w + c_3(p)\int_0^{\pi/2} dw \exp(-w/\tilde{a})w^3 + \cdots \\
&= \left[c_1(p)1!\,\tilde{a}^2 + c_3(p)3!\,\tilde{a}^4 + \cdots\right] - \tilde{a}\exp\left(-\frac{\pi}{2\tilde{a}}\right)\left[c_1(p)\left(\frac{\pi}{2}\right) + c_3(p)\left(\frac{\pi}{2}\right)^3 + \cdots\right] \\
&\quad + \mathcal{O}\left(\tilde{a}^2\exp[-\pi/(2\tilde{a})]\right) \ .
\end{aligned} \tag{A.7}$$

Incidentally, the coefficient at $\tilde{a}\exp[-\pi/(2\tilde{a})]$, written as an infinite sum, is just the value of the Borel transform at $w=\pi/2$ [cf. remark following Eq. (24)]

$$\left[c_1(p)\left(\frac{\pi}{2}\right) + c_3(p)\left(\frac{\pi}{2}\right)^3 + \cdots\right] = \left(\frac{2}{\pi}\right)\left[\left(\frac{2}{\pi}\right)^2 - \frac{1}{3}(1-p^2)\right] \ . \tag{A.8}$$

The coefficients of terms $\mathcal{O}\left(\tilde{a}^2\exp[-\pi/(2\tilde{a})]\right)$ can be obtained in an analogous manner, by using derivatives of the Borel transform with respect to w at $w=\pi/2$. Expressions (A.7)–(A.8) show explicitly the following: In the small–$\tilde{a}$ expansion of $\mathrm{Re}\delta\tilde{\mathcal{L}}_0$ of (6), in addition to the usual perturbation expansion part (11) that is analytic at $\tilde{a}=0$, we obtain formally also terms $\sim\tilde{a}^n\exp[-\pi/(2\tilde{a})]$ which are nonanalytic at $\tilde{a}=0$. One might suspect that such terms could possibly be of nonperturbative origin, and below we will show that they are not. More specifically, we will show that they are an artifact of the abruptness of the IR cutoff and that they are de facto not there, in the sense that they disappear when we consider instead of $\mathrm{Re}\delta\tilde{\mathcal{L}}_0$ its numerical equivalent, i.e., the $\varepsilon \to +0$ limit of the left–hand side of (A.6). To show this, we have to expand the latter expression [at $\varepsilon \neq 0$ – i.e. (A.1)] around $\tilde{a}=0$. For that, we first Taylor–expand the regulator $\rho_\varepsilon(w)$ (A.4), which is analytic everywhere,[7] in powers of w for small ε

$$\tilde{\rho}_\varepsilon(w) = \tilde{\rho}_\varepsilon(0) - w\,\frac{\varepsilon}{2}\left(\frac{2}{\pi}\right)^3 - \cdots - w^n\,\frac{\varepsilon}{2}\left(\frac{2}{\pi}\right)^{n+2} - \cdots + \mathcal{O}(\varepsilon^3) \ , \tag{A.9}$$

$$\tilde{\rho}_\varepsilon(0) = 1 - \frac{2}{\pi}\varepsilon + \mathcal{O}(\varepsilon^3) \ . \tag{A.10}$$

---

[7] In contrast to the abrupt cutoff when $\rho_0(w)=1$ for $w<(\pi/2)$, and $\rho_0(w)=0$ for $w>(\pi/2)$.

The other part of the integrand in (A.1), without the exponent, is the Borel transform whose small–$\tilde{a}$ expansion is (22) with $\tilde{a} \mapsto w$. Combining this and (A.9)–(A.10), we obtain after some straightforward algebra[8] the small–$\tilde{a}$ expansion of (A.1) around $\tilde{a}=0$ for small ε

$$\begin{aligned}
&\mathrm{Re}\delta\tilde{\mathcal{L}}_{\varepsilon}^{(\mathrm{P.})}(\tilde{a};p)^{(\mathrm{exp.})} = \Big[c_1(p)1!\,\tilde{a}^2 + c_3(p)3!\,\tilde{a}^4 + c_5(p)5!\,\tilde{a}^6\cdots\Big] \\
&-\varepsilon\frac{1}{2}\left(\frac{2}{\pi}\right)^3\Bigg\{c_1(p)2!\,\tilde{a}^3 + \left(\frac{2}{\pi}\right)c_1(p)3!\,\tilde{a}^4 \\
&+\left[\left(\frac{2}{\pi}\right)^2 c_1(p) + c_3(p)\right]4!\,\tilde{a}^5 + \left[\left(\frac{2}{\pi}\right)^3 c_1(p) + \left(\frac{2}{\pi}\right)c_3(p)\right]5!\,\tilde{a}^6 \\
&+\left[\left(\frac{2}{\pi}\right)^4 c_1(p) + \left(\frac{2}{\pi}\right)^2 c_3(p) + c_5(p)\right]6!\,\tilde{a}^7 + \cdots\Bigg\} + \mathcal{O}(\varepsilon^2)\ . \qquad \text{(A.11)}
\end{aligned}$$

Here we see explicitly that the small–$\tilde{a}$ expansion of $\mathrm{Re}\delta\tilde{\mathcal{L}}_{\varepsilon}^{(\mathrm{P.})}(\tilde{a};p)$ of (A.1) at nonzero ε exists and that this function is analytic there, having no nonanalytic terms $\sim\exp(-\mathrm{const.}/\tilde{a})$, in contrast to the expansion of $\mathrm{Re}\delta\tilde{\mathcal{L}}_0$ where ε was set equal to zero exactly (i.e., inside the integral). Further, expansion (A.11) goes over into the usual perturbation expansion $\delta\tilde{\mathcal{L}}^{\mathrm{pert.}}$ (11) when $\varepsilon\to+0$.

These considerations thus lead us to the following conclusions:

- The perturbative part of the induced Lagrangian density, $\mathrm{Re}\delta\tilde{\mathcal{L}}_0$ as defined in (6), has an abrupt IR cutoff at $w=\pi/2$, and it is numerically equal to the corresponding expression with an infinitesimally softened IR cutoff – cf. left–hand side of (A.6).

- The small–$\tilde{a}$ expansion of $\mathrm{Re}\delta\tilde{\mathcal{L}}_0(\tilde{a};p)$ reproduces the usual perturbation expansion (11) plus nonanalytic terms $\sim\tilde{a}^n\exp(-\mathrm{const.}/\tilde{a})$ [cf. (A.7)].

- The small–$\tilde{a}$ expansion of the corresponding expression (A.1) with a softened IR cutoff ($\varepsilon\neq 0$) yields no nonanalytic terms; when the softening of the IR cutoff becomes infinitesimal ($\varepsilon\to+0$, $\varepsilon\neq 0$), the expansion becomes identical with that of the usual perturbation expansion (11).

- The above points show that the nonanalytic terms in the small–$\tilde{a}$ expansion of $\mathrm{Re}\delta\tilde{\mathcal{L}}_0(\tilde{a};p)$ are only an artifact of the abruptness of the IR cutoff (the cutoff regulator becomes a nonanalytic function of the proper time w) and are thus not of a nonperturbative physical origin. $\mathrm{Re}\delta\tilde{\mathcal{L}}_0(\tilde{a};p)$ should be reinterpreted as the limit with the infinitesimally softened IR cutoff [the left–hand side of (A.6)], the latter being numerically the same but its small–$\tilde{a}$ expansion having no nonanalytic terms.

[8] We again integrate term–by–term; and we repeatedly use the identity: $\int_0^\infty du\exp(-u)u^n = n!$.

REFERENCES

[1] W. Heisenberg and H. Euler, *Z. Physik* **98**, 714 (1936);

[2] V. Weisskopf, *Kgl. Danske Videnskab. Selskabs. Mat.-fys. Medd.* **14**, No. 6 (1936).

[3] J. Schwinger, *Phys. Rev.* **82**, 664 (1951).

[4] W. Greiner, B. Müller, and J. Rafelski, *Quantum electrodynamics of strong fields*, 594 pp. (Berlin, Heidelberg, Springer 1985);

[5] W. Dittrich and M. Reuter, *Effective Lagrangians in Quantum Electrodynamics*, 244 pp. (Springer 1985).

[6] J. Schwinger, *Particles, Sources and Fields*, Vol. II, 306 pp., Chapters 4–8 (Addison–Wesley, 1989).

[7] C. Itzykson and J.-B. Zuber, *Quantum Field Theory*, 705 pp., Chapter 4-3 (McGraw-Hill, New York, 1980).

[8] I. A. Batalin, S. G. Matinyan, and G. K. Savvidy, *Sov. J. Nucl. Phys.* **26**, No. 2, 214 (1977).

[9] R. Ragazzon, *Phys. Rev.* **D52**, 2422 (1995).

[10] P. Schwab, *Phys. Lett.* **B109**, 47 (1982).

[11] A. B. Migdal and S. B. Khokhlachev, *Pis'ma Zh. Eksp. Teor. Fiz.* **41**, No. 4, 159 (1985) [*JETP Lett.* **41**, No. 4, 194 (1985)].

[12] V. I. Ritus, *Zh. Eksp. Teor. Fiz.* **69**, 1517 (1975) [*Sov. Phys. JETP* **42**, 774 (1976)]; V. I. Ritus, *Zh. Eksp. Teor. Fiz.* **73**, 807 (1977) [*Sov. Phys. JETP* **46**, 423 (1977)]; V. I. Ritus, *Effective Lagrange function of intense electromagnetic field in QED*, in Proceedings of the conference *Frontier tests of QED and physics of the vacuum*, pp. 11–28, Sandansky, Bulgaria, June 1998, eds. E. Zavattini, D. Bakalov and C. Rizzo (Heron Press, Sofia, 1998), also hep-th/9812124.

[13] M. Reuter, M. G. Schmidt, and C. Schubert, *Ann. Phys. (N.Y.)* **259**, 313 (1997).

[14] G. V. Dunne and C. Schubert, *Nucl. Phys.* **B564**, 591 (2000)

[15] F. Sauter, *Z. Phys.* **69**, 742 (1931); *ibid* **73**, 547 (1931).

[16] O. Klein, *Z. Phys.* **53**, 157 (1929).

[17] A. I. Nikishov, *Zh. Eksp. Teor. Fiz.* **57**, 1210 (1969) [*Sov. Phys. JETP* **30**, 660 (1970)].

[18] A. Casher, H. Neuberger, and S. Nussinov, *Phys. Rev.* **D20**, 179 (1979).

[19] D. L. Burke *et al.*, *Phys. Rev. Lett.* **79**, 1626 (1997). The electron pair production measurement reported in this work included, beside several soft ("homogeneous") laser photons, one energetic Compton–backscattered photon. The latter photon thus probes the field inhomogeneity since its wavelength is much smaller than that of the laser field.

[20] Z. Białynicka-Birula and I. Białynicki-Birula, *Phys. Rev.* **D2**, 2341 (1970).

[21] S. L. Adler, *Ann. Phys. (N.Y.)* **67**, 599 (1971).

[22] E. Brezin and C. Itzykson, *Phys. Rev.* **D3**, 618 (1971).

[23] W.-Y. Tsai and T. Erber, *Phys. Rev.* **D10**, 492 (1974); *ibid* **12**, 1132 (1975).

[24] W. Dittrich and H. Gies, *Phys. Rev.* **D58**, 025004 (1998); W. Dittrich and H. Gies, *Vacuum birefringence in strong magnetic fields*, in Proceedings of the conference *Frontier tests of QED and physics of the vacuum*, pp. 29–43, Sandansky, Bulgaria, June 1998, eds. E. Zavattini, D. Bakalov and C. Rizzo (Heron Press, Sofia, 1998), also hep-th/9806417.

[25] D. Bakalov *et al.*, *PVLAS: Vacuum birefringence and production and detection of nearly*

massless, weakly coupled particles by optical techniques, *Nucl. Phys. B Proc. Suppl.* **35**, 180 (1994).
[26] S. A. Lee *et al.*, *Measurement of the magnetically–induced QED birefringence of the vacuum and an improved laboratory search for light pseudoscalars*, FERMILAB-PROPOSAL-P-877A, 1998.
[27] G. Cvetič, private notes.
[28] R. D. Peccei, J. Solà, and C. Wetterich, *Phys. Rev.* **D37**, 2492 (1988).
[29] George A. Baker, Jr. and Peter Graves–Morris, *Padé Approximants*, 2nd edition, 746 pp. (Encyclopedia of Mathematics and Its Applications, Vol. 59), edited by Gian-Carlo Rota (Cambridge University Press, 1996).
[30] A. H. Mueller, *Nucl. Phys.* **B250**, 327 (1985); V. I. Zakharov, *Nucl. Phys.* **B385**, 452 (1992); A. I. Vainshtein and V. I. Zakharov, *Phys. Rev. Lett.* **73**, 1207 (1994); *ibid* **75**, 3588E (1995); M. Beneke, *Phys. Rept.* **317**, 1 (1999) and references therein.
[31] C. B. Chiu and S. Nussinov, *Phys. Rev.* **D20**, 945 (1979), cf. especially Fig. 1 there.
[32] P. A. Rączka, *Phys. Rev.* **D43**, R9 (1991).
[33] M. Pindor, hep-ph/9903151.
[34] U. D. Jentschura, *Phys. Rev.* **D62**, 076001 (2000).
[35] G. V. Dunne and T. M. Hall, *Phys. Rev.* **D60**, 065002 (1999).
[36] U. D. Jentschura, J. Becher, E. J. Weniger, and G. Soff, hep-ph/9911265.
[37] M. Beneke and V. M. Braun, *Phys. Lett.* **B348**, 513 (1995); P. Ball, M. Beneke and V. M. Braun, *Nucl. Phys.* **B452**, 563 (1995); Y. L. Dokshitzer, G. Marchesini, and B. R. Webber, *Nucl. Phys.* **B469**, 93 (1996); E. Gardi and G. Grunberg, *JHEP* **11**, 016 (1999).
[38] S. G. Matinyan and G. K. Savvidy, *Nucl. Phys.* **B134**, 539 (1978).
[39] E. Gardi, G. Grunberg, and M. Karliner, *JHEP* **07**, 007 (1998); F. A. Chishtie, V. Elias, V. A. Miransky, and T. G. Steele, hep-ph/9905291.
[40] R. D. Ball, *Phys. Rep.* **182**, 1 (1989); G. Cvetič, *Ann. Phys. (N.Y.)* **255**, 165 (1997).

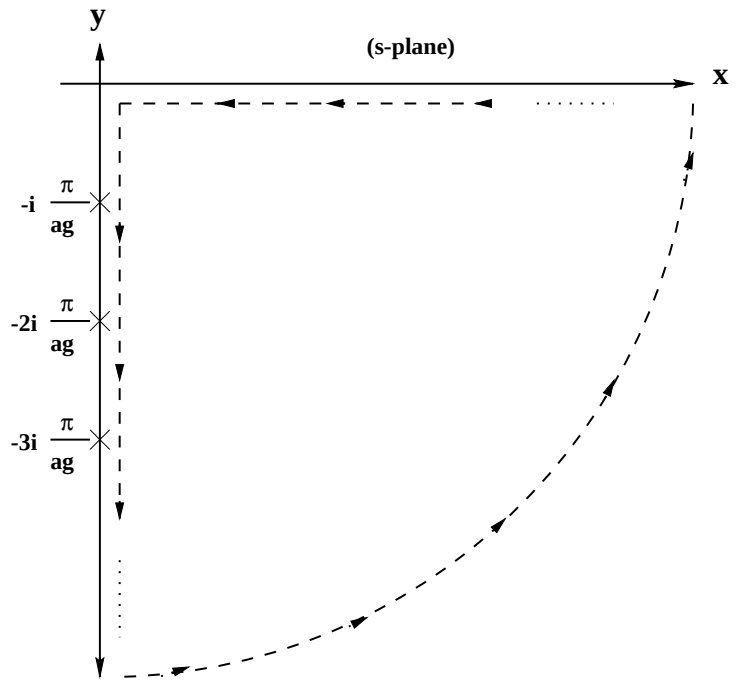

FIG. 1. The contour integration, in the complex s–plane, needed to rewrite (1) in the form (4). The location of the poles is denoted explicitly.

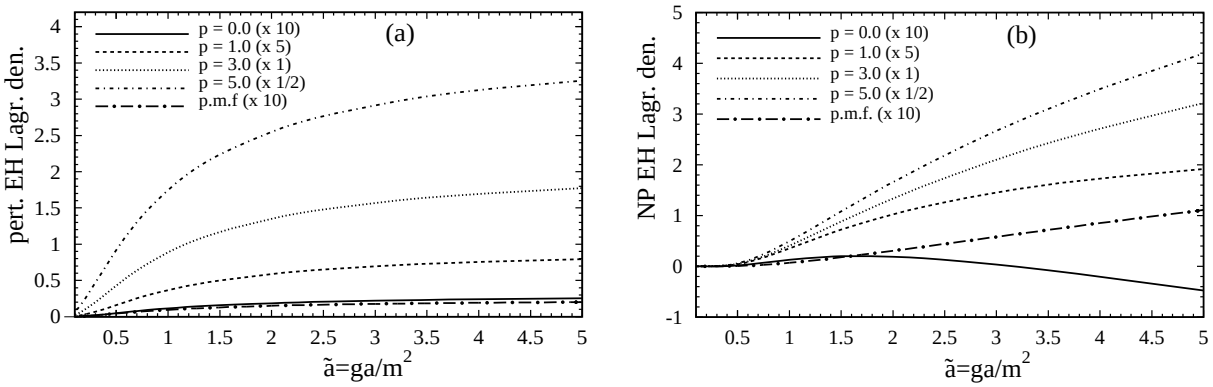

FIG. 2. (a) Perturbative and (b) nonperturbative induced dispersive (Euler–Heisenberg) Lagrangian densities [cf. (6) and (7)] as functions of the (quasi)electric field parameter $\tilde{a}$ (8), at various fixed values of the magnetic–to–electric field ratio $p=\tilde{b}/\tilde{a}$ (8). The actual values of the curves for $p\approx 0$, $p=1.0$ and $p=5.0$ have been multiplied here by factors 10, 5 and 1/2, respectively, for better visibility. Included is also the case of the pure (quasi)magnetic field (p.m.f.), for which the x-axis represents $\tilde{b}=gb/m^2$.

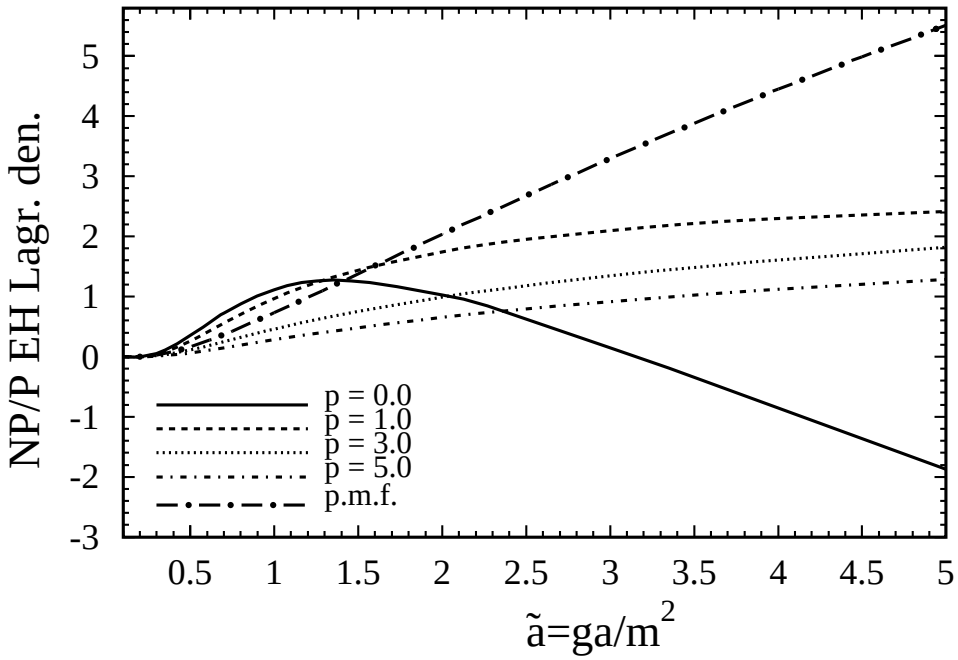

FIG. 3. Ratios of the nonperturbative and the perturbative induced dispersive Lagrangian densities for the cases depicted in Figs. 2. For the p.m.f. case, the x-axis represents $\tilde{b}=gb/m^2$.

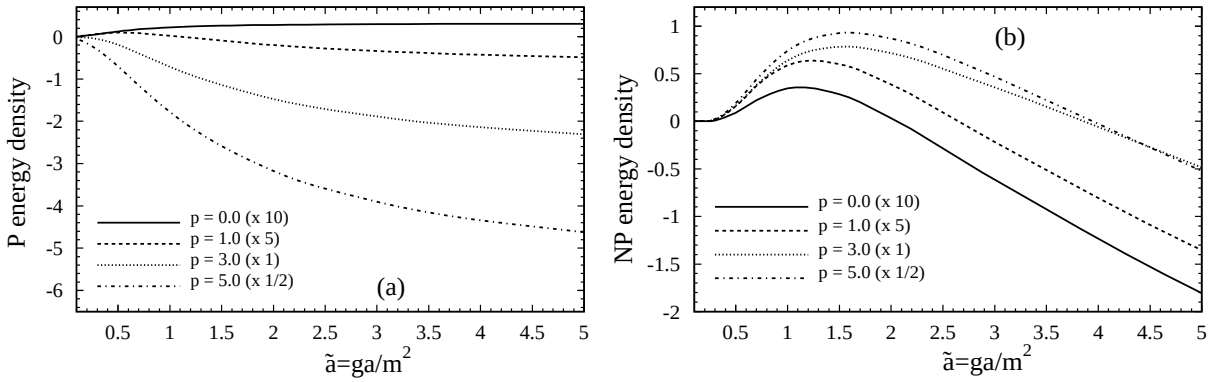

FIG. 4. (a) Perturbative and (b) nonperturbative induced energy densities [cf. (16) and (17)] as functions of $\tilde{a}$ at various fixed values of $p = \tilde{b}/\tilde{a}$ (8). The actual values of the curves have been multiplied, for better visibility, by the denoted factors, just as in Figs. 2.

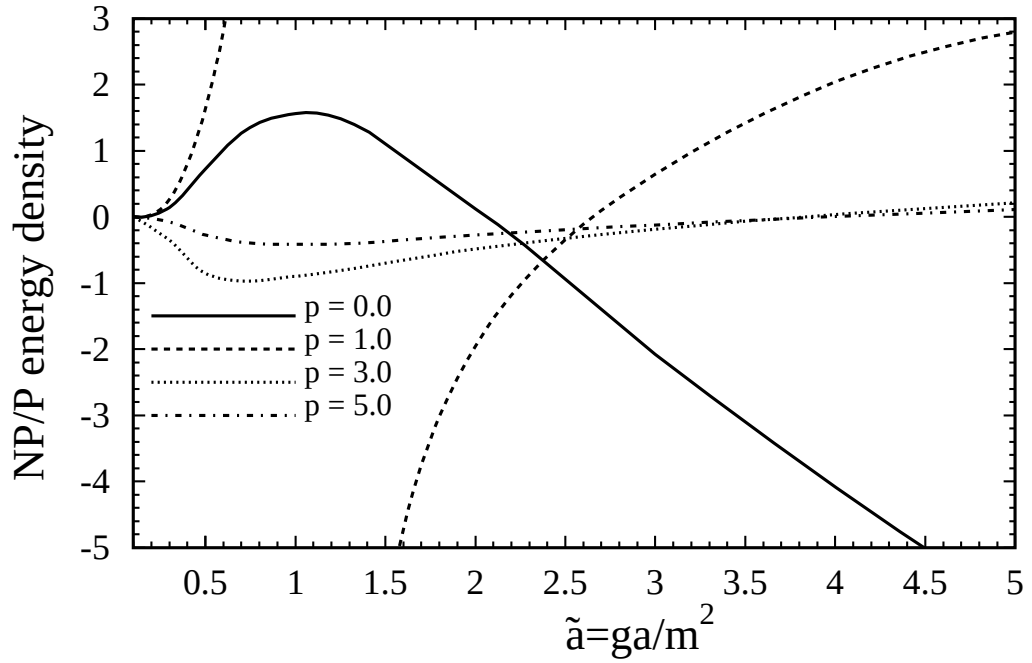

FIG. 5. Ratios of the nonperturbative and the perturbative induced energy densities for the cases depicted in Figs. 4. The ratio for $p = 1$ varies strongly for $\tilde{a} = 0.5$–1.5 because the perturbative induced density has a zero at $\tilde{a} \approx 1.1$.

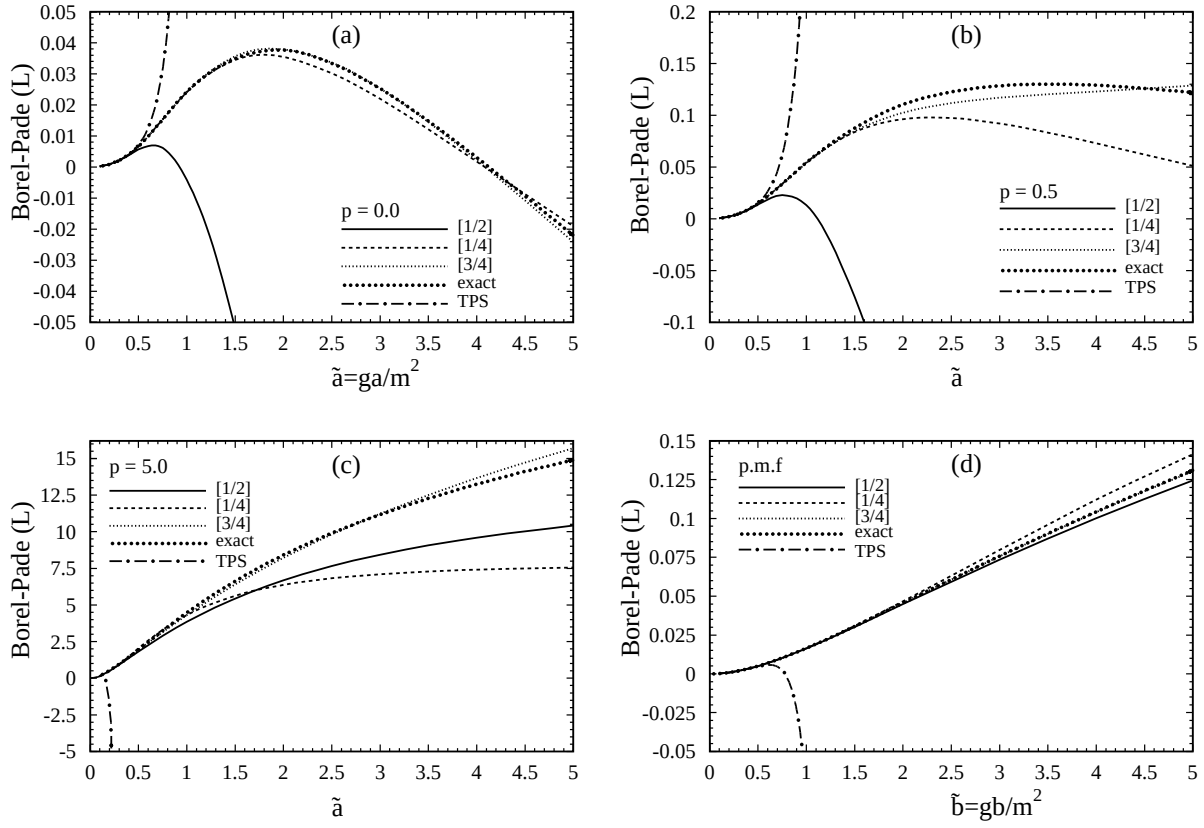

FIG. 6. Borel–Padé approximants (BP's) to the induced dispersive Lagrangian density (8) as functions of $\tilde{a}$, for various values of $p=\tilde{b}/\tilde{a}$: (a) $p=0$; (b) $p=0.5$; (c) $p=5.0$; (d) pure magnetic field ($\tilde{a}=0$). Depicted are those BP's (23) which are based on the Padé approximants [1/2], [1/4] and [3/4] of the Borel–transform (22). The numerically exact curves [sum of curves of Figs. 2 (a) and (b)] are also included and they virtually agree with the [3/4] BP results. Included are also the the results of the truncated perturbative series which include terms $\sim\tilde{a}^8$ [in (d): $\sim\tilde{b}^8$].

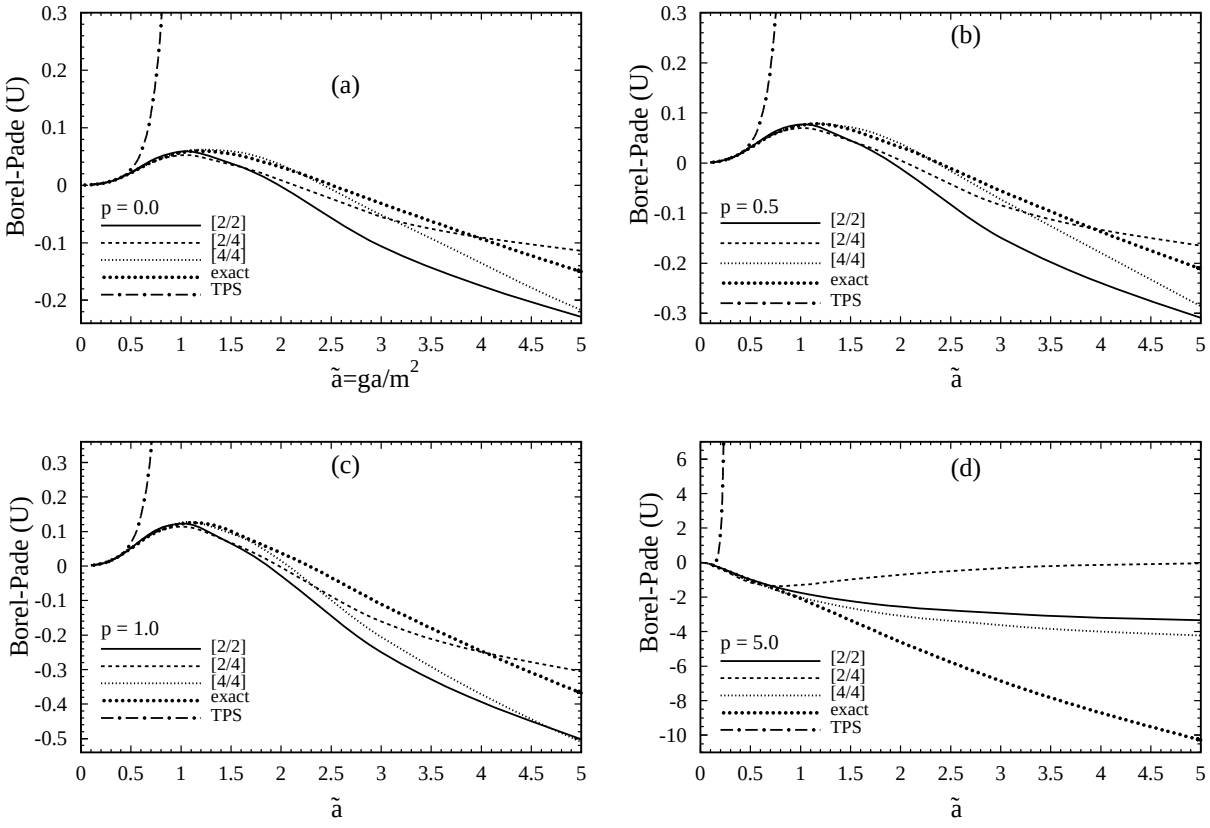

FIG. 7. Modified Borel–Padé approximants [MBP's – cf. (28)] to the induced energy densities, based on the Padé approximants [2/2], [2/4] and [4/4] for the MBP's (27), as functions of $\tilde{a}$, at fixed values of $p=\tilde{b}/\tilde{a}$: (a) $p=0$; (b) $p=0.5$; (c) $p=1.0$; (d) $p=5.0$.